Catena 217 (2022) 106517

Contents lists available at ScienceDirect

Catena

journal homepage: www.elsevier.com/locate/catena

Mineralogical association and geochemistry of potentially toxic elements in urban soils under the influence of mining

Annika Parviainen [a,b,*], Antón Vázquez-Arias [c], Francisco José Martín-Peinado [a]

[a] Departamento de Edafología y Química Agrícola, Universidad de Granada, Avda. Fuente Nueva s/n, E-18071 Granada, Spain
[b] Instituto Andaluz de Ciencias de la Tierra (UGR-CSIC), Avda. de las Palmeras 4, E-18100 Armilla, Granada, Spain
[c] CRETUS Institute, Departamento de Biología Funcional, Universidade de Santiago de Compostela, Santiago de Compostela, Spain

ARTICLE INFO

Keywords:
Arsenian plumbojarosite, beudantite
Soil geochemistry
Environmental mineralogy
Mining area

ABSTRACT

Polluted soil is an important source of exposure to potentially toxic elements (PTEs) for humans, especially in urban areas. We studied the fate of PTEs in the total (<2 mm) and fine (<50 μm) fractions of urban soils in playgrounds, passing areas, and vacant lots of the historic mining village of Minas de Riotinto in SW Spain. The mineralogical and chemical observations included analysis by scanning electron microscopy, electron backscatter diffraction, X-ray diffraction, chemical analysis of Al, V, Cr, Mn, Co, Ni, Cu, Zn, Rb, Sr, As, Cd, Ba, Tl, and Pb after acid digestion by Inductively Coupled Plasma-Mass Spectrometry and Sb by X-ray fluorescence.

The total and fine fractions of natural and mixed (consisting of natural soils and aggregate pavements) urban soils have significantly higher concentrations of sulfide-associated PTEs (Ni, Cu, Zn, As, Sb, and Pb) and Ba in comparison to the aggregate pavements. Most of the natural and mixed urban soils surpass the regulatory levels set by the regional Government for As and Pb to declare a soil as contaminated. This work highlights the mineralogical source of PTEs in the urban soils. Primary geogenic sulfide minerals are prone to oxidation promoting dissolution of PTEs and acid generation in the future. Additionally, for the first time, we have described arsenian plumbojarosite and beudantite in urban soils which are abundant secondary phases under the circumneutral pH conditions, effectively retaining As and Pb. Inhalable small PTE-rich particles (<10 μm) are present in many soils in playgrounds and garden areas potentially posing health risk to residents upon dusting and resuspension in the air.

1. Introduction

Urban soils represent around 3% of the global terrestrial surface, but more than half of the world's population is concentrated in urban areas. Hence, the influence of urban soils on human health is a growing concern (Li et al., 2018), especially for children (Han et al., 2020). Humans transiting public areas are exposed to pollution of potentially toxic elements (PTEs) from urban soils via inhalation, ingestion, and dermal contact (Li et al., 2018). Children are more vulnerable for hazardous substances in comparison to adults (Zhang et al., 2019). According to (Fernández-Navarro et al., 2017, 2012), the proximity of mining and related industries increases the mortality rate associated to certain types of cancer in Spain. There are also indications that residents in mining areas are at higher risk of developing pigment gallstones in comparison to a control population and that these calculi are enriched in sulfide-associated PTEs (Parviainen et al., 2018, 2016).

Soil geochemistry is mainly influenced by parent rock lithology and mineralizations (Galán et al., 2008), but also by the contribution of soil forming processes and human activities (Díez et al., 2009). Therefore, urban soils of cities located in mining regions may be enriched in PTEs due to natural processes (ore deposit lithology) and anthropogenic activities (mining).

Atmospheric pollution derived from mining activities and related industries is known to have a negative impact on the surrounding soils (Ettler, 2015). When these activities are located nearby residential areas, they may have an impact on urban soils (Alsaleh et al., 2018; Argyraki et al., 2018). Mine waste sites are usually barren which promotes the resuspension of fine particulate matter (PM) in the atmosphere. Furthermore, according to their size, airborne PM from polluted soils or mine wastes can be divided into solid particles suspended by wind, ranging between 1 and 100 μm, and other aerosols smaller than 1 μm, and may be dispersed in the air (U.S.EPA, 1996; WHO, 2000). Fine

* Corresponding author at: Departamento de Edafología y Química Agrícola, Universidad de Granada, Avda. Fuente Nueva s/n, E-18071 Granada, Spain.
E-mail addresses: aparviainen@ugr.es (A. Parviainen), anton.vazquez.arias@rai.usc.es (A. Vázquez-Arias), fjmartin@ugr.es (F.J. Martín-Peinado).

https://doi.org/10.1016/j.catena.2022.106517
Received 9 May 2022; Received in revised form 27 June 2022; Accepted 4 July 2022

airborne PM may be transported over long distances and deposited in urban areas (Csavina et al., 2012). Hence, deposition of airborne PM may alter the mineralogical and chemical composition of urban soils by accumulation of sulfide minerals, associated to mine wastes, and their alteration products.

So far, little attention has been paid to the quality of urban soils and their potential impact on human health in the mining towns located in Huelva Province, SW Spain. Dozens of towns, including for instance Minas de Riotinto, Nerva, El Campillo, La Dehesa, Tharsis and Calañas, were built close to mines that were active in the past century. The human health risk is mainly related to the potential increase of cancer risk and other chronic toxic effects by the cumulative potential of carcinogenic and non-carcinogenic elements from polluted urban soils (Fernández-Caliani, 2012; Zhang et al., 2019). Recently, we reported on the carcinogenic risk of natural urban soils of Minas de Riotinto for As and Pb and increased cancer mortality rates in this locality for neoplasms associated with these elements (Parviainen et al., 2022). Our current study aims to characterize the mineralogical-chemical association of PTEs in different types of urban soils (natural and aggregate fillings) in Minas de Riotinto, which are key indicators of potential pollution and health risk to residents in areas close to mining activities, using a multidisciplinary approach combining soil science, environmental geochemistry, and mineralogy. Minas de Riotinto offers a unique study site due its location in the proximity of one of the World's largest non-ferrous metal reserves, where large-scale mining activities date back to 19th century and earliest activities to 3rd Millenium BC (Nocete et al., 2014). We aimed to study the bulk mineralogy and chemistry as well as the characteristics of the soil fine fractions (<50 μm) in relation to the different parent materials and soil use, as a first step to assess the environmental and potential human health risk of the urban soils. This study provides essential information for the local decision makers in choosing pavement materials in urban areas to minimize the potential exposure risk to PTEs.

2. Materials and methods

2.1. Site description

The study site, Minas de Riotinto, is located in the Province of Huelva in SW Spain (Fig. 1), where the surrounding geology is dominated by the volcano-sedimentary rocks of the Iberian Pyrite Belt that host one of the largest polymetallic massive sulfide deposits at the global level (Sáez et al., 1999; Tornos, 2006). The typical mineral assemblage in the massive sulfides consists of pyrite [FeS_2] as the main mineral phase together with sphalerite [ZnS], galena [PbS], and chalcopyrite [$CuFeS_2$] as major phases and arsenopyrite [FeAsS], tetrahedrite–tennantite [$Cu_6(Cu_4X_2^{2+})Sb_4S_{13}$–$Cu_6(Cu_4X_2^{2+})As_4S_{13}$], cobaltite [CoAsS], Sb–As–Bi sulfosalts, gold, and electrum as minor phases (Almodóvar et al., 2019). Common oxidized phases include magnetite [Fe_3O_4], hematite [Fe_2O_3], cassiterite [SnO_2], and barite [$BaSO_4$] (Almodóvar et al., 2019).

In this study, we focus on urban soils in Minas de Riotinto (approx. 4000 inhabitants), a historical mining village that was built in close vicinity of the Rio Tinto mines at the end of 19th century. The large-scale industrial mining, focusing principally on exploitation of pyrite for sulfuric acid production and copper, started in 1873, bloomed in the early 20th century, and finally ceased in 2001. Recently the mining was reactivated, and Atalaya Mining is exploiting copper since 2015 at Cerro Colorado (Fig. 1). The ceased Corta Atalaya open pit is one of the largest ones in Europe. The open pits and vast areas covered by mining residues are located to a few hundred meters from the village (Fig. 1). The historical mining residues contain for instance pyrite ashes, slag, and waste rock piles (Fernández Caliani, 2008).

Minas de Riotinto has a Mediterranean pluviseasonal oceanic bioclimate with upper thermomediterranean thermotype and low subhumid ombrotype (Rivas-Martínez et al., 2011). The annual mean temperature and precipitation are 16 °C and 603 mm, respectively (Climate-data.org, 2012). Typically, the precipitation falls between October and April. The dominant wind directions in Minas de Riotinto are N to NNE, and these winds from northerly directions blow from the mining area towards the village (Fig. 1).

2.2. Sampling

A total of thirty urban soil samples were collected from Minas de Riotinto (Fig. 1). Urban soils may be composed by natural soils developed from local parent material. Additionally, the use of aggregate materials is common in urban areas in Spain. They are made up of allochthonous materials, such as calcareous sand (known as "albero") or

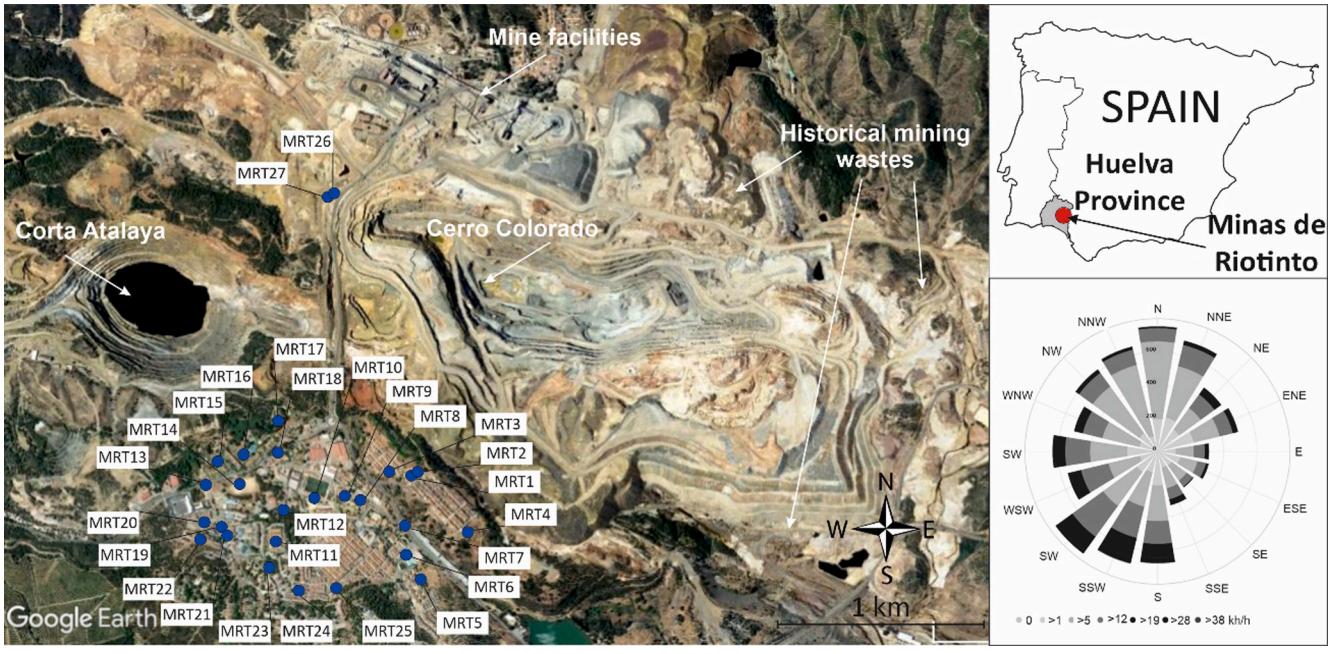

Fig. 1. Satellite image of the study area with urban soil sampling points in Minas de Riotinto (MRT) (37°41′33.3″N, 6°35′28.6″W) and a wind rose representing the wind directions (https://www.meteoblue.com).

gravel, and are usually used as fillings in pavements of parks and recreational areas. In this study we collected natural soils, and we found two types of artificially produced soils with differing characteristics, which are referred to as aggregate soils. Mixed soils refer to mixtures of natural and artificial soils. Therefore, we have classified the soil types into 1) natural; 2) calcareous sand aggregate (high-carbonate content); 3) gravel aggregate (low-carbonate content); and 4) mixed soils. The land use types are classified into 1) playground; 2) passing area; and 3) garden in public parks; and 4) vacant lots (generally used as parking lots). Football courts and a school yard are classified as playgrounds. Natural soils are usually green or vegetated areas, whereas aggregate soils do not have associated vegetation. Sample characteristics (soil type and land use) and geographical coordinates are presented in Supplementary Table S1.

Twenty seven composite topsoil samples were collected from public parks, playgrounds, and green areas representing the main urban soils available for our study. Approx. 1 kg of exposed topsoil (2–3 cm) was collected using stainless steel spatula from each sampling site from three to four points in a maximum area of 10x10 m and stored in plastic bags. Additionally, three deeper samples from 20 to 30 cm depth (assigned with letter P) were collected using soil auger corer at the sampling sites MRT4, MRT12, and MRT22 that correspond to natural soils. All sampling utensils were cleaned exhaustively in between samples with alcohol.

2.3. Sample preparation and analysis

In the laboratory, the samples were dried at room temperature applying periodic mixing. The samples were homogenized and sieved using a 2 mm mesh after which the gravel was discarded. The fraction < 2 mm was considered as total fraction. Subsequently, an aliquot of approx. 30 g was dry-sieved using a 50 μm mesh and the fine fraction (<50 μm) was recovered. The total fraction was grinded for bulk powder X-ray diffraction using PANAlytical X'PERT PRO diffractometer equipped with an X'Celerator detector and a theta-theta goniometer at the Instituto Andaluz de Ciencias de la Tierra (IACT, Granada, Spain). The measurements were performed on the scan range from 3.0 to 70.0 (2θ) with a step size of 0.0167° and time/step of 0.22 s. The identification and quantification of the mineral phases was performed using XPowder software (v. 2004.04; https://www.xpowder.com). We chose the fine fraction for further detailed mineralogical analysis because it may be subjected to airborne transport and may cause higher exposure risk to humans. The fine fraction of selected samples was mounted on carbon tape, carbon coated, and studied by FEI QemScan 650F high-resolution Field Emission Environmental Scanning Electron Microscope at Centro de Instrumentación Científica (CIC) at Universidad de Granada. Backscattered mode was used for high-resolution imaging of the fine PTE-rich particles and their semiquantitative chemical composition was studied by energy-dispersive X-ray microanalysis (EDX). The acceleration voltage was set to 20 kV for the data acquisition. For the microstructural identification of the iron oxyhydroxides and sulfate phases, two representative PTE-rich samples were chosen and silica polished probes were prepared. The carbon-coated probes were studied under AURIGA Field Emission Scanning Electron Microscope (FESEM) at CIC. The crystallographic analysis of the phases of interest was done using Electron Backscatter diffraction (EBSD) of Oxford Instruments.

Soil pH was measured in a suspension of soil total fraction and distilled water (1:2.5) using a Metrohm 914 pH/Conductometer. The suspension was agitated and let to settle for half an hour, after which pH was measured.

Both total and fine fractions of the topsoil samples were analyzed after acid digestion by an Agilent 8800 TripleQuad Inductively Coupled Plasma-Mass Spectrometry (ICP-MS) at IACT (Granada, Spain) for Al, V, Cr, Mn, Co, Ni, Cu, Zn, Rb, Sr, As, Cd, Ba, Tl, and Pb. To the exception of the topsoils samples, we analyzed only the total fraction (<2 mm) in the deep soil samples (MRT4P, MRT12P, and MRT22P), because these samples are not exposed to dusting. Samples were subjected to a microwave-assisted *aqua regia* digestion with HCl and HNO_3 (3:1). To control the quality of the analyses, a certified reference material (RTC-CRM052, loamy clay) was run and procedural blanks were analyzed to counter possible contributions from the digestion procedure. The analysis of the CRM gave satisfactory results for Al, V, Cr, Mn, Co, Ni, Zn, As, Cd, and Pb. The results for certified elements are presented in the Supplementary Table S2. Antimony was not analyzed by ICP-MS, but in the view of its importance in this study, we alternatively measured all samples by Portable X-ray Fluorescence (PXRF). RTC-CRM052 was also analyzed using PXRF in six replicates. The values for Sb were (mean 27.6 mg/kg; *standard deviation 1.5*) within the prediction interval of the certified value (20.1; *6.2*). Precision was estimated by the relative standard deviation (RSD) and the result was good (5 < RSD < 10) according to (U.S.EPA, 2006). Detection limit of PXRF for Sb is 11.7 mg/kg.

2.4. Statistical analysis

The obtained data were analyzed to verify their normal distribution and homoscedasticity, and as they were not fulfilled in all cases, nor after their logarithmic transformation, hence non-parametric tests were performed. The comparison of mean values was made using the Kruskal-Wallis test, and the analysis of the statistically significant differences between groups was made using the Mann-Whitney *U* test. The differences were considered significant when p value < 0.05. To assess the relationships between the different variables of study in the fine fraction of the soils samples, a correlation analysis (Spearman) and a Principal Component Analysis (PCA) were performed; PCA with Kaiser normalization were calculated with the components rotated using the Varimax method to clarify the relationship among factors. All statistical analyzes were made using SPSS software v.20.0 (SPSS Inc., USA).

3. Results

3.1. Bulk mineralogical composition and pH

Mineralogical composition of the major mineral phases in the soil samples is presented in Supplementary Table S3 and the data are summarized in Table 1. Evaluation of the samples by soil type reveals that natural soils in Minas de Riotinto are principally composed of quartz (average 76%) and minor amounts of other silicates, such as plagioclase, K-feldspar, muscovite and clinochlore. These natural soil samples have low neutralization potential, which is reflected by the almost total absence of carbonate minerals (only one sample, MRT4, contains 1% calcite) and the significantly lower pH values (average 6.8; Table 2) in comparison to the other soil types. The deep samples (MRT4P, MRT12P, and MRT22P) exhibit similar mineral composition with the respective natural surface samples. The calcareous sand aggregates in Minas de Riotinto contain an average 22% of quartz and are rich in carbonates with an average of 77% and 3% of calcite and dolomite, respectively. The coarser gravel aggregates contain more quartz (55%) and other silicate minerals, whereas they contain significantly less carbonates (37% and 4% of calcite and dolomite, respectively) in comparison to the calcareous sand aggregates. The pH values of the two aggregate soil types are 8.5 and 8.4, respectively. Mixed soils present higher variability in the mineralogical composition, but generally, they have higher neutralization potential than the natural soils with 17% and 42% of calcite and dolomite, respectively. The average pH of mixed soils is 8.1.

We could not distinguish any sulfide minerals or secondary mineral phases in the XRD patterns probably due to their scarcity and the restricted detection limits of the XRD mineral quantification.

3.2. Chemical composition

All analyzed elements exhibit higher median values in the fine

Table 1
Summary table of the average mineralogical composition (values in %) and standard deviations in parenthesis of major phases based on bulk powder XRD analyses in the urban soil samples from Minas de Riotinto. The soil types are classified into 1) natural; 2) calcareous sand aggregates (high-carbonate content); 3) gravel aggregates (low-carbonate content); and 4) mixed soils. (N = number of samples).

N	Soil type	Quartz	Plagioclase (Albite)	K-Feldspar (Microcline)	Muscovite	Clinochlore	Calcite	Dolomite
12	Natural soils	76 (8.7)	6.5 (5.6)	4.8 (3.2)	9.1 (5.5.)	4.8 (4.9)	1.0 (–)	–
6	Calcareous sand aggregates	21 (6.8)	3.3 (3.2)	2.0 (–)	1.3 (0.6)	–	77 (5.2)	3.0 (–)
6	Gravel aggregates	55 (6.3)	21 (5.0)	4.3 (0.6)	11 (2.6)	2.8 (0.5)	37 (18)	4.0 (–)
3	Mixed soils	44 (24)	3.7 (2.0)	1.0 (–)	6.5 (5)	2.3 (0.6)	17 (8.6)	42 (22)

fraction (<50 μm) of the urban soils in Minas de Riotinto with respect to total fraction (<2 mm; Table 2), and the difference is significant ($p < 0.05$) for V, Cr, Mn, Co, Ni, Cu, Zn, Rb, and As. The deep natural soil samples (MRT4P, MRT12P, and MRT22P) exhibit similar chemical composition with their respective surface samples, showing no significant differences for any of the analyzed elements.

The geochemical characteristics of the total and fine fractions also show trends in the PTE abundances between the different soil types (Table 2). When comparing the statistical significance of the differences in median values, we have grouped natural and mixed soils (with a natural soil component) and both types of aggregate soils. The total fractions of natural and mixed soils exhibit significantly higher concentrations of Ni, Cu, Zn, As, Ba, and Pb in comparison to aggregate soils. The fine fractions of natural and mixed soils contain significantly higher concentrations of Ni, Cu, Zn, As, Ba, Tl, and Pb in comparison to aggregate soils, whereas higher values of V and Sr in aggregate soils.

We pay special attention to the chemical composition of the soil fine fraction because there is a higher risk of inhalation of fine particles. The elements associated to sulfide minerals present significantly higher median values including Cu (235 and 370 mg/kg, respectively), Zn (223 and 125 mg/kg), As (272 and 263 mg/kg), and Pb (882 and 536 mg/kg) in the fine fractions of natural and mixed soils in comparison to the total fractions (Table 2). Additionally, these soils exhibit elevated median values for Ba with 465 and 502 mg/kg, respectively. The natural soils exhibit high chemical variation with elevated standard deviation values (Table 2), probably due to variability in the geological units and mineralizations. Because of the high detection limit of Sb by PXRF in comparison to ICP-MS, we were able to detect Sb only in the samples that have high concentrations of other sulfide-associated elements (including six natural samples MRT3, MRT4, MRT13, MRT18, MRT 24, and MRT27; two mixed samples MRT15 and MRT26; and two aggregate samples MRT10 and MRT17). For instance, the highest concentrations of As, Sb, and Pb in natural soils correspond to a playground (MRT24; 1950 mg/kg, 271 mg/kg, and 6370 mg/kg, respectively), whereas in mixed soils the highest concentrations are found in a garden soil of a public park (MRT15; 2660 mg/kg, 445 mg/kg, and 9749 mg/kg, respectively). Additionally, the samples from the Cerro Colorado viewpoint (MRT26 and MRT27) –closest to the mining area– exhibit high concentrations in the fine fraction for Cu (6750 and 2090 mg/kg, respectively), Zn (1020 and 233 mg/kg), As (193 and 519 mg/kg), Sb (60 and 147 mg/kg), and Pb (422 and 1170 mg/kg).

Both types of aggregate soils, in general, exhibit lower concentrations of all determined elements, except for V and Sr that are present at significantly higher median concentrations than in the natural and mixed soils (Table 2). The low-carbonate aggregates exhibit similar median values to natural soils for Rb. However, high concentrations of PTEs related to sulfide minerals are found in the fine fraction of only one aggregate soil sample with high carbonate content (MRT17 in a passing area) with up to 293 mg/kg of As, 36 mg/kg of Sb, and 789 mg/kg of Pb.

3.3. Mineralogical characteristics of PTEs

Observations under electron microscope revealed clear differences in the abundances of PTE-bearing phases between natural and artificial aggregate soils (Supplementary Fig. S1). In Minas de Riotinto, the fine fractions of the natural and mixed soils contained abundant primary sulfide minerals, as well as abundant secondary mineral phases containing PTEs (Figs. S1A-B). On the contrary, the calcareous soils contain very scarce PTE-bearing grains (Figs. S1C-D).

Detailed observations on the natural soils in Minas de Riotinto affirm the presence of abundant primary minerals such as galena and barite. Additionally, less abundant mineral phases of geogenic origin, such as ilmenite [$FeTiO_2$], well-crystalline Fe oxide (hematite and magnetite) and cassiterite, are found. Besides primary mineral phases, different secondary minerals are observed, which are formed as consequence of sulfide oxidation. Abundant Fe hydroxide phases (goethite [$Fe^{3+}O(OH)$] and ferrihydrite [$Fe_2^{3+}O_3 \bullet 0.5(H_2O)$]) retain SO_4 and PTEs with varying concentrations of As (approx. 1.3–2.5 wt%), Sb (1.5–3.1 wt%), Cu (0.6–1.1 wt%), and Pb (1.2–2.7 wt%), and also some grains are void of PTEs (Fig. 2A,D). Arsenian plumbojarosite [$Pb_{0.59}Fe_3(AsO_4)_{0.18}(SO_4)_{1.82}(OH)_6$] and beudantite [$PbFe_3(AsO_4)(SO_4)(OH)_6$] are also abundant in the natural soils, for instance in the sample MRT24 located in a playground (Fig. 2C,D). These phases contain traces of Cu (0.7–1.7 wt%). An unidentified Sn and Sb-rich phase (approx. 28 and 19 wt%, respectively) with Fe (20.0 wt%) and traces of As, S, and Pb is also detected (Fig. 2C). These secondary mineral phases are found as agglomerations of small crystals covering other mineral phases, as well as abundant single crystals (<5 μm) (Fig. 2). The mineral identification by crystallographic analysis using EBSD confirmed the presence of goethite, ferrihydrite, plumbojarosite, and beudantite (Supplementary Fig. S2), as well as geogenic phases including magnetite, hematite, galena, and sphalerite. Beudantite and plumbojarosite tend to appear together as fine-grained aggregates as shown in Figure S2.

The PTE-rich mineral phases found in mixed soil samples in Minas de Riotinto are similar to those in natural soils. They contain small grains (<5 μm) of primary sulfide minerals, such as galena, sphalerite, and pyrite. Moreover, abundant geogenic barite and well-crystalline Fe oxide, and less abundant zircon [$ZrSiO_4$], monazite [$(CeLaNd)PO_4$], and celestine [$SrSO_4$] are observed. The secondary phases encountered include Fe hydroxides (goethite and ferrihydrite), arsenian plumbojarosite, and beudantite (Fig. 3; Fig. S2). The Fe hydroxides are abundant and usually found coating surfaces of silicate mineral grains. In MRT1 –a mixed calcareous sand sample located in a playground– these secondary phases do not retain PTEs perceivable to SEM-EDX (Fig. 3A). Whereas, in MRT15 –located in a garden area of a public park– Fe hydroxides retain traces of Cu, As, Sn, Sb, and Pb (Fig. 3B). Abundant arsenian plumbojarosite and beudantite occur coating other minerals and as small (<3 μm) individual grains in the mixed soils located in gardens (Fig. 3B,C,D; Supplementary Fig. S1), and beudantite is found to trap Cu (approx. 1.0–1.9 wt%), Sb (4.5 wt%), and Sn (4.1 wt%; Fig. 3C,D).

The calcareous sand type of aggregate samples in passing areas of public parks in Minas de Riotinto have only scarce PTE-bearing phases (Fig. S1). A few sulfide mineral grains are found, including chalcopyrite, galena, pyrite, and also an unidentified Pb phosphate. A few grains of well-crystalline Fe oxides, barite, monazite, ilmenite, and zircon are also found. Scarce Fe hydroxides contain in some cases Zn (2.3–6.7 wt%; MRT17 in Fig. 4A) or As and Pb (MRT10; Fig. 4B), as well as, seldom As, Sn, Sb, and Pb. Additionally, scarce aggregates of arsenian plumbojarosite and beudantite, void of PTEs perceivable to ESEM-EDX, presenting hexagonal crystal forms (MRT8 and MRT10; Fig. 4D,E) and Mn-Fe

Table 2
Summary table of the pH values and chemical composition (mg/kg) of the urban soils in Minas de Riotinto classified by soil type 1) natural; 2) calcareous sand aggregates (high-carbonate content); 3) gravel aggregates (low-carbonate content); and 4) mixed soils. (N = number of samples; SD = standard deviation; T = total fraction; F = fine fraction).

	pH	Al		V		Cr		Mn		Co		Ni		Cu		Zn		Rb		Sr		As		Cd		Ba		Tl		Pb	
		T	F	T	F	T	F	T	F	T	F	T	F	T	F	T	F	T	F	T	F	T	F	T	F	T	F	T	F	T	F
Natural soils (N = 12)																															
Mean	6.8	12,400	44,800	25	41	18	38	211	396	3.7	7.0	11	21	380	576	143	206	28	41	64	45	324	420	1.4	1.1	393	667	0.48	0.77	842	1370
Median	7.1	11,200	38,800	20	46	16	41	159	444	2.8	8.0	9.0	24	89	235	82	223	23	42	28	43	78	272	0.63	0.57	167	465	0.41	0.62	208	882
SD	1.4	6430	26,000	18	18	14	17	151	220	2.4	2.5	7.1	10	864	776	134	100	19	14	132	32	414	540	1.9	1.1	383	645	0.34	0.51	1080	1740
Min.	3.6	5890	24,300	5.6	9.4	2.3	6.1	23	60	1.1	1.5	1.6	3.3	11	55	25	25	8.3	17	8.7	12	6.2	43	0.09	0.38	52	112	0.06	0.23	34	82
Max.	8.5	26,600	120,700	61	61	42	58	495	833	8.6	10	27	33	3090	2270	431	346	78	62	479	132	1050	1950	4.2	3.4	1180	2340	0.98	1.9	3320	6370
Calcareous sand aggregates (N = 6)																															
Mean	8.5	3250	14,510	36	88	16	39	201	442	3.1	7.0	4.6	13	22	47	98	147	7.2	17	155	193	50	93	0.11	0.31	54	132	–	0.22	83	167
Median	8.5	2760	14,220	36	97	16	41	191	416	2.5	6.2	3.7	12	10	29	41	53	6.3	17	164	215	23	52	0.11	0.19	33	68	–	0.22	16	26
SD	0.16	1250	3650	9.0	21	4.5	8.0	68	74	1.7	2.1	2.2	2.1	23	44	142	220	2.5	4.3	37	49	54	99	–	0.30	47	128	–	0.11	151	307
Min.	8.3	2290	8690	27	46	10	24	129	378	1.9	5.5	2.2	10	5.9	18	14	39	5.2	9.5	98	117	21	34	<0.00	0.11	27	63	<0.00	0.11	10	18
Max.	8.7	5570	18,500	50	100	24	47	327	574	6.5	11	7.7	16	62	133	382	594	12	22	191	237	156	293	0.11	0.74	148	385	<0.00	0.33	389	789
Gravel aggregates (N = 6)																															
Mean	8.4	7870	29,900	21	46	11	28	364	675	2.3	4.2	4.9	12	31	94	36	61	26	39	229	104	15	34	0.10	0.47	106	142	0.16	0.21	24	48
Median	8.4	8970	32,500	21	42	8.9	25	282	532	2.0	4.0	3.2	12	25	84	34	53	33	35	55	78	14	32	0.10	0.47	70	88	0.16	0.18	14	36
SD	0.30	4520	17,400	14	34	9.2	14	258	512	1.2	1.2	4.4	5.3	19	53	21	31	16	30	419	98	8.1	17	–	0.16	97	116	0.07	0.17	20	45
Min.	8.0	2120	8200	5.9	13	2.3	9.1	98	205	1.1	2.5	2.2	5.9	11	33	12	31	4.4	9.7	8.5	19	5.8	17	<0.00	0.36	22	43	0.091	0.035	8.7	17
Max.	8.8	12,200	49,700	35	85	26	50	775	1550	4.6	6.0	14	20	57	176	68	115	40	89	1080	268	25	53	0.10	0.59	270	347	0.22	0.46	60	137
Mixed soils (N = 3)																															
Mean	8.1	5820	26,100	19	44	17	33	1090	1570	5.0	11	10	15	951	2410	175	420	13	21	194	74	1260	1040	0.90	1.3	787	737	0.25	0.49	3390	3570
Median	8.0	5350	22,300	15	35	11	36	1270	1770	3.6	6.3	6.2	15	352	370	93	125	16	23	107	74	113	263	0.87	0.54	240	502	0.32	0.52	159	536
SD	0.22	3060	19,600	9.2	31	15	19	903	454	4.6	9.4	7.5	3.3	1350	3760	203	523	6.3	12	214	42	2080	1400	0.8	1.6	1090	649	0.17	0.12	5720	5350
Min.	7.9	3030	8750	12	19	5.7	12	106	1050	2.1	4.9	4.8	11	7.5	115	26	109	5.7	8.7	37	31	2.6	193	0.31	0.32	75	238	0.05	0.36	16	422
Max.	8.3	9090	47,400	29	79	35	50	1880	1890	11	22	18	18	2490	6750	406	1020	17	32	438	116	3660	2660	1.4	3.2	2050	1470	0.36	0.60	10,000	9740

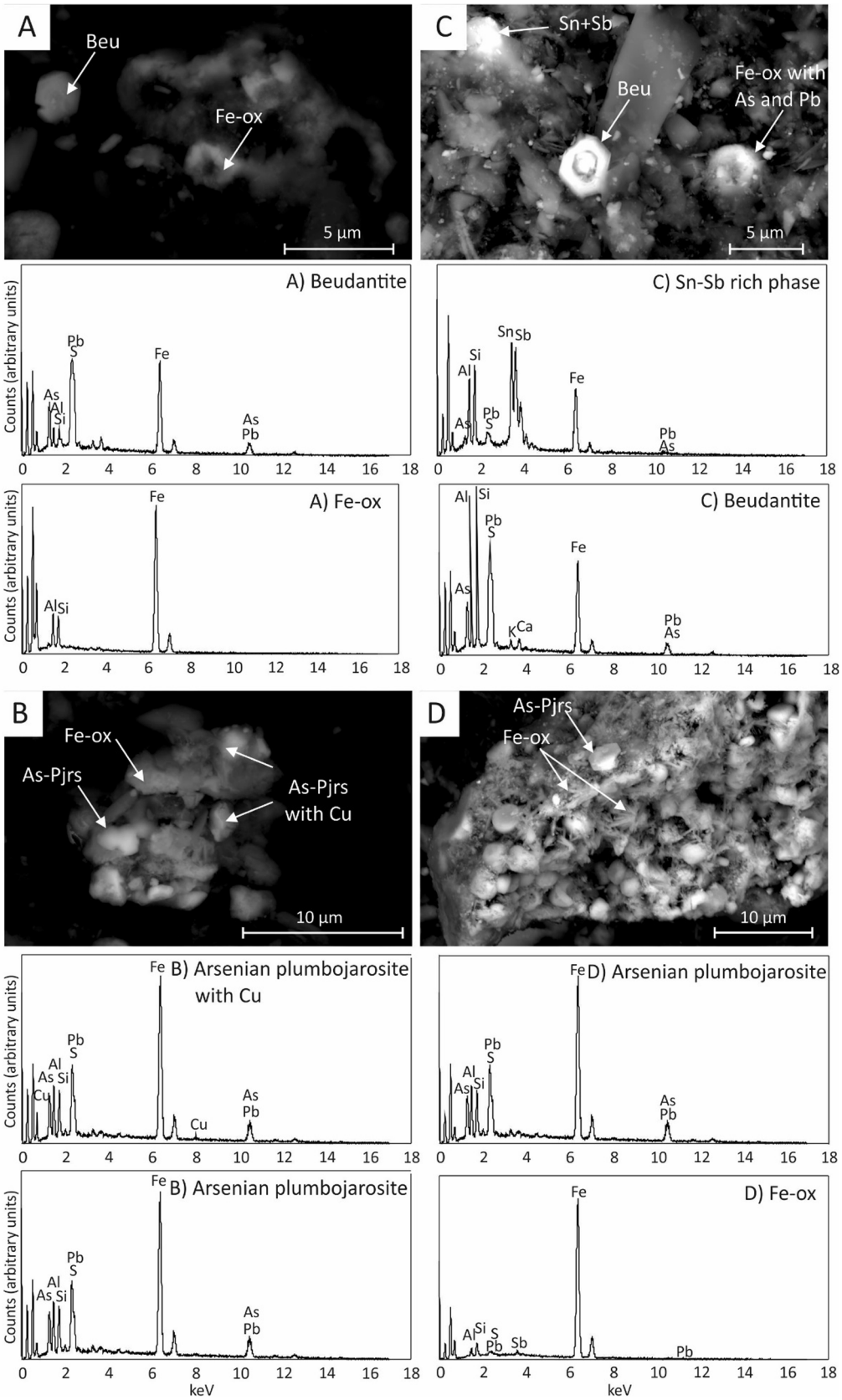

Fig. 2. Backscattered images of natural soils in Minas de Riotinto. A) Beudantite (Beu) and Fe hydroxide (MRT4), B) arsenian plumbojarosite (Pjrs) and Fe hydroxide (MRT4), C) a Sn and Sb –rich phase and beudantite (MRT24), D) arsenian plumbojarosite and Fe hydroxide (MRT24).

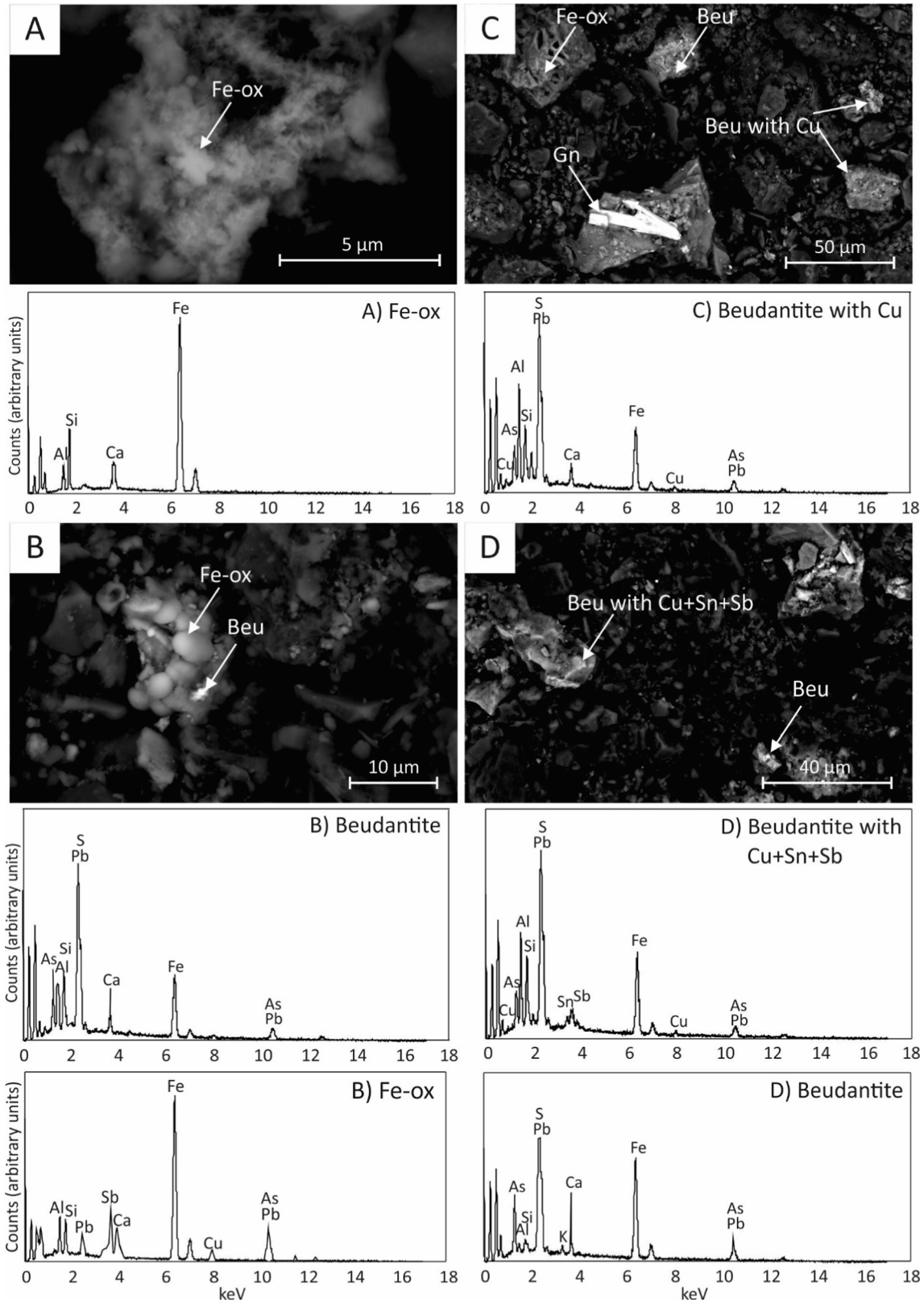

Fig. 3. Backscattered images of mixed soils in Minas de Riotinto. A) Fe hydroxide (MRT1), B) beudantite (Beu) and Fe hydroxide (MRT15), C) galena (Gn), beudantite and Fe hydroxide (MRT15), and D) beudantite of varying composition (MRT15).

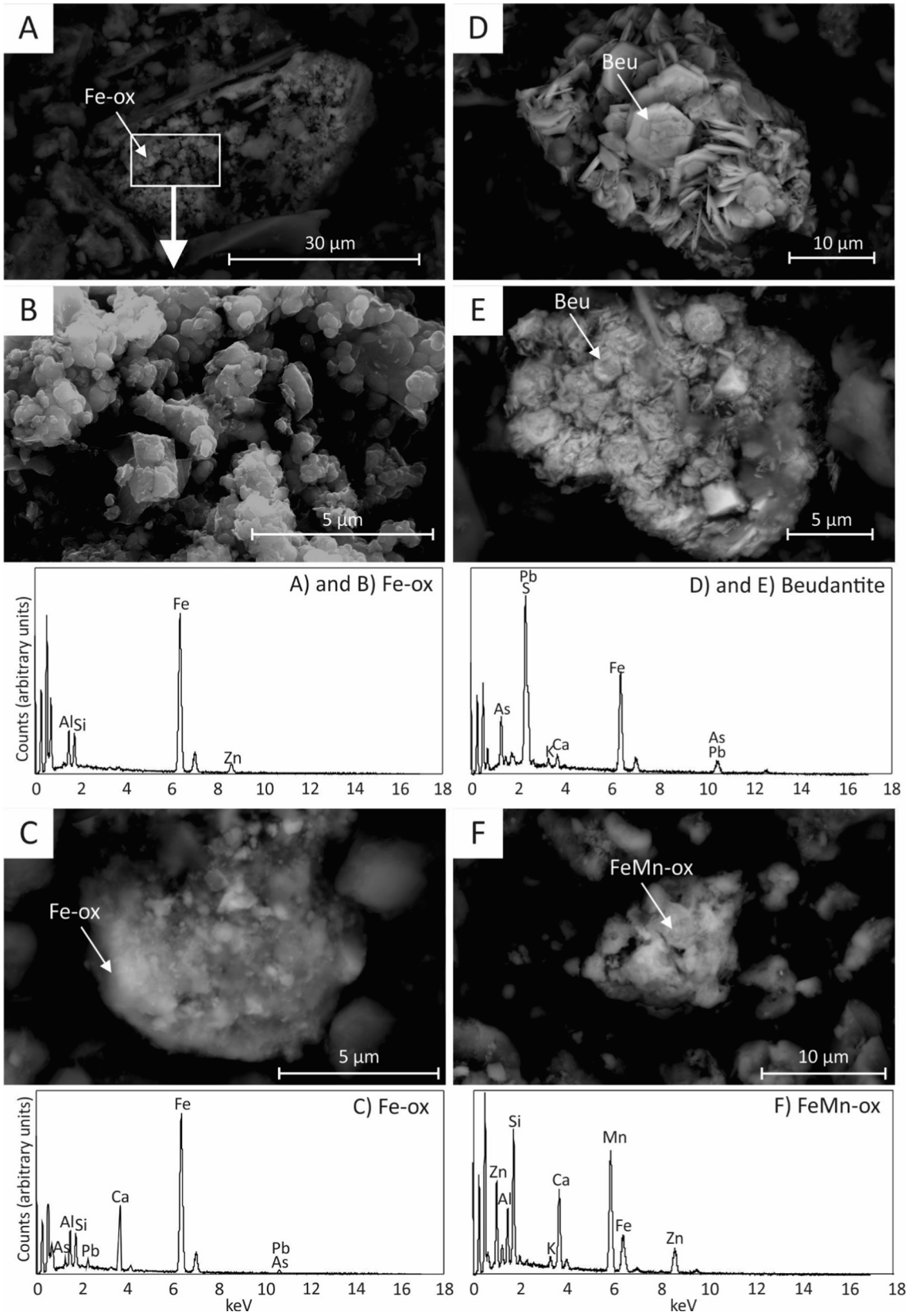

Fig. 4. Backscattered images of aggregate soils in Minas de Riotinto. A) Fe hydroxide with Zn (MRT10), B) a detailed photo of the Fe hydroxide, C) Fe hydroxide with As and Pb (MRT17), D) and E) beudantite (Beu; MRT8) and F) Fe-Mn(oxy)hydroxide (MRT10).

Table 3
Results of Spearmans's correlations for fine fraction of natural and mixed urban soils in Minas de Riotinto.

	Al	V	Cr	Mn	Co	Ni	Cu	Zn	Rb	Sr	As	Cd	Ba	Tl	Pb
Al	1.000	0.835**	0.721**	−0.229	0.395	0.357	−0.514*	0.082	0.123	0.357**	−0.318	−0.206	−0.339	−0.246	−0.268
V		1.000	0.831**	0.233	0.441	−0.036	−0.322	0.213	0.077	0.732**	−0.088	−0.073	−0.227	−0.196	−0.039
Cr			1.000	0.202	0.468	0.066	−0.261	0.233	−0.047	0.701**	−0.102	0.224	−0.157	−0.178	0.079
Mn				1.000	0.261	−0.643**	0.218	0.171	0.150	0.518*	0.289	0.222	0.139	−0.039	0.336
Co					1.000	0.278	0.193	0.470	0.019	0.361	0.352	0.178	0.349	0.190	0.426
Ni						1.000	−0.084	0.179	−0.118	−0.269	−0.158	0.164	−0.005	−0.040	−0.195
Cu							1.000	0.593*	−0.059	−0.089	0.693**	0.596*	0.721**	0.679**	0.600*
Zn								1.000	0.107	0.289	0.254	0.523*	0.314	0.301	0.182
Rb									1.000	−0.290	−0.379	−0.013	−0.143	−0.108	−0.382
Sr										1.000	0.154	0.159	−0.025	−0.276	0.236
As											1.000	0.149	0.886**	0.711**	0.936**
Cd												1.000	0.293	0.094	0.186
Ba													1.000	0.642**	0.818**
Tl														1.000	0.679**
Pb															1.000

**Correlation is significant at the 0.01 level (2- tailed).
*Correlation is significant at the 0.05 level (2-tailed).

hydroxide with traces of Zn (MTR10; Fig. 4F) are found. These secondary phases also appear as small crystals < 3 μm.

4. Discussion

4.1. Mineral-chemical association of PTEs in urban soils

The bulk mineralogical composition of the urban soils in Minas de Riotinto shows contrasting patterns between natural soils with high quartz contents and artificial aggregate soils with high carbonate contents, whereas mixed soils have highly varying quartz, calcite, and dolomite contents (Table 1 and Table S3). Subsequently, the median pH value of natural soils is significantly lower than that of aggregate soils. Based on the chemical abundance and mineralogical characteristics of the PTEs, Cu, Zn, As, Sn, Sb, Ba, and Pb are recognized as the most relevant PTEs in the urban soils, whereas other PTEs, such as, Co, Cr, Ni, and Cd are found in lower concentrations (Table 2). A recent study on the soils surrounding the nearby town of El Campillo, revealed similar trends with, on the one hand, large variation and high concentrations of As (min.-max. 7.0–2230 mg/kg), Cu (13–1120 mg/kg), Pb (19–3490 mg/kg), and Zn (18–722 mg/kg), and on the other hand, smaller variation and lower concentrations of Co (0.4–96 mg/kg), Cr (0.60–268 mg/kg), Ni (1.4–95 mg/kg), and Cd (0.020–3.3 mg/kg) (Zuluaga et al., 2017). These authors established background values for soils of El Campillo for Cr (21 mg/kg), Co (14 mg/kg), Ni (20 mg/kg), Cu (83 mg/kg), Zn (93 mg/kg), As (45 mg/kg), Cd (0.16 mg/kg), and Pb (89 mg/kg), which may serve as background values for Minas de Riotinto as the distance between the towns is three kilometers and they host similar lithology. The mean values of natural and mixed soils of Minas de Riotinto surpass these background values for Cu (380 and 951 mg/kg, respectively), Zn (143 and 175 mg/kg), As (324 and 1257 mg/kg), Pb (842 and 3392 mg/kg), and slightly for Cd (1.4 and 0.90 mg/kg), but not for Cr (18 and 17 mg/kg), Co (3.7 and 5.0 mg/kg), and Ni (11 and 10 mg/kg). We also compared the mean concentrations of the deep natural soil samples with the background values from El Campillo. Copper (97 mg/kg), As (446 mg/kg) and Pb (587 mg/kg) presented higher values than the background. These observations suggest the lithological association of the anomalous concentrations of PTEs (including Cu, As, Zn, and Pb) in the natural urban soils. These elements are directly associated with minerals in the ore deposit (Almodóvar et al., 2019; Sáez et al., 1999). The mean values of all aggregate soils do not exceed the background values set by Zuluaga et al. (2017). When comparing median values, only As, Cu, and Pb (as well as Cd slightly) surpass the background values for natural and mixed soils. Furthermore, according to the regulatory values set by the Decree of Andalusian Government, most of

Table 4
Results of PCA for fine fraction of urban soils in Minas de Riotinto. The Kaiser-Meyer-Olkin value was 0.5. The correlations with high factor loadings are highlighted with bold numbers.

	1	2	3
Al	0.159	−0.096	−0.241
V	−0.185	**0.890**	−0.236
Cr	0.207	**0.750**	−0.169
Mn	0.229	−0.017	**0.673**
Co	0.405	0.437	−0.129
Ni	0.007	−0.646	−0.339
Cu	0.022	−0.265	**0.861**
Zn	0.034	−0.166	**0.828**
Rb	−0.002	−0.520	0.474
Sr	−0.322	**0.843**	−0.150
As	**0.936**	0.042	0.068
Cd	0.078	−0.082	**0.802**
Ba	**0.927**	−0.149	0.114
Tl	**0.580**	−0.500	0.040
Pb	**0.925**	0.055	0.076
Variability	31%	20%	15%

the soils may be declared as potentially contaminated (Decreto 18/2015, 2015). The majority of studied natural (70% with median 73 mg/kg of As and 50% with median 208 mg/kg of Pb in total fraction; Table 2) and mixed urban soils (67% with median 113 mg/kg of As and 30% with median 159 mg/kg of Pb) surpass this regulatory value for As (36 mg/kg) and Pb (275 mg/kg). Only one aggregate soil sample exceeds the regulatory values for both As and Pb (MRT17 with 156 and 389 mg/kg, respectively), whereas another sample exceeds the value for As (MRT8 with 52 mg/kg).

Among the studied elements, Cr, Cd, As, Ni, and Pb are recognized as toxic to humans, and, according to the International Agency for Research on Cancer, Cr (VI), Ni, As, Cd, and Pb are carcinogenic and Sb is potentially carcinogenic to humans (IARC, 1989; Tchounwou et al., 2012). Furthermore, the pH is a key factor controlling the fate of PTEs in soils (Simón et al., 2005). Therefore, understanding the mineralogical associations of PTEs and their potential mobility is essential in an urban environment to assess the toxicity of these soils.

Spearman's correlations of the fine fraction of the natural and mixed soils show, on the one hand, that As presents very high positive correlation with Pb (0.94) which is strongly supported by the presence of abundant arsenian plumbojarosite and beudantite in these soils (Table 3). Additionally, Cu, As, Ba, Tl, and Pb present high positive pairwise correlations (0.60–0.89). Zinc is positively and highly correlated with Cu (0.60), whereas moderately correlates with Cd (0.53). Further, Sr presents high positive correlations with V (0.73) and Cr (0.70), and Cr with V (0.83), whereas Mn correlates with Ni (0.64). Rubidium does not correlate with any of the other elements. When Spearman's correlations are run for all urban soils together, the results are very similar to natural soils –exhibiting very high positive correlation for the main pollutants including Cu, As, Ba, Tl, and Pb, and additionally Zn presents positive correlation with these elements.

The PCA performed on the fine fraction of the urban soils in Minas de Riotinto includes three components explaining 66% of the variability (Table 4). Component 1 (explaining 31%) includes As, Ba, and Pb (and Tl with weaker factor loading) in direct relationship; Component 2 (explaining 20%) includes V, Cr, and Sr also in direct relationship; and Component 3 (explaining 15%) includes Mn, Cu, Zn, and Cd. Cobalt and Rb have weak factor loadings. According to these groups, Component 1 (elements with lower mobility) and Component 3 (recognized as micronutrients with higher mobility; (Kabata-Pendias, 2010) seem to be related to the main pollutants, *i.e.*, to the elevated concentrations of PTEs found in these samples. Arsenic and Pb are sulfide-associated elements found in the ore deposit (Almodóvar et al., 2019). The Component 2 is related to elements that exhibit low concentrations in the natural soils. All statistical analyses imply the association of Ba with the main sulfide-related elements (*e.g.,* As and Pb), however, Ba merely occurs in barite. Even though there is no mineralogical association, the compositional abundances of Ba correlate with sulfide-related elements in the natural and mixed soils. We did not include Sb in the PCA due to the different techniques used for the chemical analysis. However, we find high Sb concentrations in samples with high concentrations of As and Pb. Subsequently, Sb shows very high correlation with As (0.92) and Pb (0.91) in these samples. Additionally, mineralogical analysis confirmed that Sb is related to sulfide-associated elements, such as As, Sn, and Pb.

Arsenian plumbojarosite and beudantite are common secondary phases after alteration of primary sulfide minerals (such as galena) described in mining environments. They appear as natural alteration products of ore deposits and also in mine wastes, but are rarely described in urban soils (to our knowledge this is the first time they are described in urban soils). For instance, beudantite works as a natural sink for As and Pb in gossans in the Iberian Pyrite Belt (Nieto et al., 2003), and it has been detected in tailings in various mine sites working as a natural attenuation mechanism for As and Pb (Courtin-Nomade et al., 2016, 2002; Gieré et al., 2003; Kocourková et al., 2011; Néel et al., 2003; Romero et al., 2010, 2007; Roussel et al., 2000). Beudantite was also detected in agricultural soils in Taiwan and was reported to have low solubility in the same pH range as in the natural soils of Minas de Riotinto (Chiang et al., 2010). Leaching tests at pH 2 and 4 also exhibited low solubility of As and Pb (Chiang et al., 2010). Our study shows that these minerals, that are common oxidative weathering products of galena (Nieto et al., 2003), are abundant in urban soils of Minas de Riotinto, especially in the natural and mixed soils, but are also detected in the aggregate soils (Figs. 2-4). Arsenopyrite, tedrahedrite, and As-Sb sulfosalts are primary sources of As and Sb in the massive sulfide deposits of the Iberian Pyrite Belt (Almodóvar et al., 2019). Beudantite and plumbojarosite act as important traps for As and Pb which explains the high correlation between these elements, but As, Cu, Zn, Sb, and Pb are also retained by Fe hydroxides in trace amounts (generally below 3.0 wt % for each element; Figs. 2-4).

Hexagonal plumbojarosite $[Pb_{0.5}Fe_3^{3+}(SO_4)_2(OH)_6]$ and beudantite belong to the alunite supergroup –a large group of minerals with varying compositions– and are stable in the pH conditions of the studied soils presenting low solubility with solubility products (K_{sp}) from 10^{-15} to 10^{-21} (Forray et al., 2014; Kocourková et al., 2011; Kolitsch and Pking, 2001; Roussel et al., 2000). Beudantite and plumbojarosite form solid-solutions and they present high crystal-chemical flexibility being able to incorporate different elements (*e.g.,* Cu and Sb) (Hudson-Edwards, 2019; Kolitsch and Pking, 2001; Pekov et al., 2016; Sejkora et al., 2009). In our study, we find traces of Cu, Sn, and Sb in beudantite (Fig. 3C,D). Studies on synthetic As-Pb jarosite with pseudo-rhombohedral morphology also suggest that these phases immobilize effectively As and Pb and are potential long-term traps (Forray et al., 2014).

The remaining sulfide minerals in the natural and mixed soils are prone to oxidation in the atmospheric conditions prevailing in the topsoils. Hence, they may contribute to the liberation of PTEs, further acidification of soils, and subsequent precipitation of secondary phases. The fate of PTEs in the precipitating secondary phases depends on the dynamics between Fe^{3+}, SO_4^{2-}, and soil properties (Simón et al., 2002). In the pH range of the studied soils, goethite and ferrihydrite are stable phases with K_{sp} values from 10^{-37} to 10^{-41}, even though decreasing crystal size and Al substitution may increase the K_{sp} by several orders of magnitude (Bigham et al., 1996; Schwertmann, 1991). Hence, the presence of Fe hydroxides, beudantite and plumbojarosite, pH, and soil properties, play key roles in the fate of As, Cu, Zn, Sb, and Pb, that may be prone to remobilization after mineral dissolution in case of changing pH and redox conditions (Simón et al., 2005, 2002). The Fe hydroxides detected in the current study represent less important long-term traps for As and Pb in comparison to for instance beudantite, because they contain lower concentrations of these PTEs. The mobility and availability of most divalent cationic metals decrease at higher soil pH, whereas the mobility of oxyanions (including As and Sb) gradually increases with rising pH (McLean and Bledsoe, 1992). Arsenic is a redox sensitive element (Couture et al., 2015) that is readily mobilized under anoxic conditions in soils, but here in oxidized surface environment As tends to be stable.

4.2. Influence of particle size on the potential exposure risk of PTEs

Based on our study, the natural and mixed urban soils of Minas de Riotinto contain higher amounts of PTEs in comparison to artificial soils, and both total and fine fractions of the natural and mixed soils have significantly higher concentrations of Ni, Cu, Zn, As, Ba, and Pb. Accordingly, recent studies report elevated concentrations of Cu, As, and Pb in the topsoils of the nearby village of El Campillo (Zuluaga et al., 2017) and in sediments of the Tinto River affected by mining (Cruz-Hernández et al., 2016; Parviainen et al., 2015), as well as high contents of Cu and Pb in mine soils (Monaci et al., 2020; Rossini-Oliva et al., 2016). Our mineralogical observations under scanning electron microscope reveal that PTEs are mainly associated to particles < 10 μm, including both primary, geogenic mineral phases such as sulfides, as well as, secondary phases, including arsenian plumbojarosite,

beudantite, and Fe hydroxides. This study also highlights that smaller (<5 μm) PTE-bearing particles are frequent in the natural and mixed soils, and to lesser extent in aggregate materials. Even though, the mineralized parent rocks have a major influence on the chemical and mineralogical composition of the natural soils (Galán et al., 2008), the enrichment of sulfide-associated PTEs, and especially As, in some aggregate soils of Minas de Riotinto implies that deposition of atmospheric PM derived from the mining site may contribute to the quality of the urban soils. The calcareous aggregates are poor in PTEs by nature therefore we assume that higher concentrations come from an external source. In fact, Co, Ni, Cu, As, and Pb present significantly higher values in the fine fraction of aggregate soils with respect to the total fraction, which implies the deposition of airborne PM. However, we cannot rule out other processes, and the elevated PTE concentrations in artificial soils may be affected by admixing of aggregate fillings with surrounding and underlaying natural soils even though there may not be apparent disturbance. Recent studies, however, corroborate that the contaminated soils and mining facilities in the Rio Tinto mining district is a persistent source of atmospheric pollution of PTEs (Castillo et al., 2013; Fernández-Caliani et al., 2013; Sánchez de la Campa et al., 2020). According to these authors, the windblown PM (<10 μm) has similar chemical and mineralogical characteristics to the mine wastes. The airborne PM adjacent to the mine waste dumps contains sulfide-related PTEs, including As, Bi, Cd, Cu, Sb, Zn, and Pb. Pyrite, chalcopyrite, and their secondary phases such as goethite, jarosite, plumbojarosite, and hematite, were detected (Fernández-Caliani et al., 2013). Additionally, they detected apatite [$Ca_5(PO_4)_3F$], gypsum [$CaSO_2{\cdot}2H_2O$], ilmenite, rutile [TiO_2], titanite [$CaTi(SiO_4)O$], cassiterite, zircon, and monazite as minor phases in the PM. The airborne PM from mine sites may cause direct exposure risk to humans. Additionally, deposition of PM may influence the quality of the urban soils by altering their chemical and mineralogical composition.

During the hot and dry summer season, as is the case in our study area, windblown dust and resuspension of fine PM of polluted urban soils may pose a severe exposure risk to residents via inhalation. Children – while playing – may additionally be exposed through ingestion and dermal contact. Based on our health risk assessment of the urban soils of Minas de Riotinto, considering the whole town of as an exposure area, the studied soils exhibit carcinogenic risk of As for both adults and children, whereas As and Pb present non-carcinogenic risk for children (Parviainen et al., 2022). Many studies have reported that the smaller fractions, PM < 10 μm and especially < 2.5 μm, pose higher exposure risk via inhalation, because these particles may penetrate and deposit deeper in the lungs to the trachea-bronchial or alveolar area (Oberdörster et al., 2005; Schlesinger et al., 2006; Valavanidis et al., 2008; Zereini et al., 2012). Furthermore, other studies have estimated PTE bioaccessibility from geogenic PM in lungs using in-vitro studies that simulate lung fluids. For instance, (Guney et al., 2017) suggested high bioaccessibility for PTEs, such as As, Cu, Fe, Mn, Ni, Pb, and Zn, from PM derived from contaminated soils and mine tailings. The chemical form of the inhaled PM influences on the bioaccessibility and toxicity of PTEs on humans (González-Grijalva et al., 2019; Mazinanian et al., 2013). Furthermore, the mineralogical composition of the soils may have an impact on the gastric bioaccessibility of As (Meunier et al., 2010; Morais et al., 2019). Hence, identifying the mineralogical-chemical characteristics of the small particles is important in urban soils to evaluate potential exposure risk to PTEs. The results of this study may have an implication in choosing the pavement material for public areas to minimize exposure risk to humans. Calcareous sands or gravel pavements have proven as better options in comparison to natural soils in Minas de Riotinto. However, further toxicity assays and bioaccessibility tests are necessary to comprehensively evaluate the potential toxicity of the urban soils in Minas de Riotinto.

5. Conclusions

For the first time, the mineralogical-chemical association of PTEs in the urban soils of Minas de Riotinto in SW Spain is studied in this work, and we evaluated the characteristics of the soil total and fine fractions in the view of potential exposure risk to humans. Natural soil development in the mineralized bedrock area of the Iberian Pyrite Belt results in significantly higher concentrations of Ni, Cu, Zn, As, Sb, Ba, and Pb in both total and fine fractions of the natural and mixed (with natural soil component) urban soils in comparison to the artificial aggregate soils. The fine fraction of aggregate soils, that are composed of calcareous sand and by nature do not exhibit elevated contents of PTEs, serve us in evaluating the deposition of anthropogenic airborne PM derived from the mining area.

This work highlights the mineralogical control of PTEs in the urban soils. The remaining, unweathered sulfide minerals may be a source of soluble PTEs upon oxidation in the future, whereas abundant arsenian plumbojarosite and beudantite are stable mineral phases under the pH conditions of the studied soils and serve as important traps for As and Pb. The PTEs are commonly present in the small particles (<10 μm) that may be inhalable upon dusting and suspension in the air.

This study also highlights the importance of the selection of pavement material of urban areas that are overlying mineralized bedrock. The natural and mixed soils of Minas de Riotinto contain anomalous concentrations of PTEs, especially Cu, As, Sb, and Pb. Many of the old playgrounds in Minas de Riotinto were constructed on natural soils and the ones having calcareous sand pavements have been worn down mixing with the underlying natural soil (*e.g.* MRT1, MRT9, MRT18, and MRT24). In these cases, covering the natural soils by calcareous sands would improve the quality of the urban soils and decrease the PTEs' exposure risk to humans.

Declaration of Competing Interest

The authors declare that they have no known competing financial interests or personal relationships that could have appeared to influence the work reported in this paper.

Acknowledgements

We would like to acknowledge Ms. I. Martínez Segura and Mr. M.J. Roman Alpiste for their assistance in laboratory work. We also acknowledge the different funding sources. Dr. A. Parviainen's fellowship 'Juan de la Cierva –Incorporación' (IJCI-2016-27412) was funded by the Spanish Ministry of Science, Innovation and Universities. The research performed at the UGR was also supported by the Research Project RTI 2018-094327-B-I00 (Ministry of Science, Innovation and Universities). Fellowships, research and infrastructure grants supporting this research performed at the Instituto Andaluz de Ciencias de la Tierra (UGR-CSIC) have been (co)funded by the European Regional Development Fund (ERFD) and the European Social Fund (ESF) of the European Commission. This work received funding for open access charge: Universidad de Granada / CBUA.

Appendix A. Supplementary material

Supplementary data to this article can be found online at https://doi.org/10.1016/j.catena.2022.106517.

References

Almodóvar, G.R., Yesares, L., Sáez, R., Toscano, M., González, F., Pons, J.M., 2019. Massive sulfide ores in the iberian pyrite belt: Mineralogical and textural evolution. Minerals 9 (11), 653. https://doi.org/10.3390/min9110653.

Alsaleh, K.A.M., Meuser, H., Usman, A.R.A., Al-Wabel, M.I., Al-Farraj, A.S., 2018. A comparison of two digestion methods for assessing heavy metals level in urban

soils influenced by mining and industrial activities. J. Environ. Manage. 206, 731–739. https://doi.org/10.1016/j.jenvman.2017.11.026.
Argyraki, A., Kelepertzis, E., Botsou, F., Paraskevopoulou, V., Katsikis, I., Trigoni, M., 2018. Environmental availability of trace elements (Pb, Cd, Zn, Cu) in soil from urban, suburban, rural and mining areas of Attica, Hellas. J. Geochem. Explor. 187, 201–213. https://doi.org/10.1016/j.gexplo.2017.09.004.
Bigham, J.M., Schwertmann, U., Traina, S.J., Winland, R.L., Wolf, M., 1996. Schwertmannite and the chemical modeling of iron in acid sulfate waters. Geochim. Cosmochim. Acta 60 (12), 2111–2121. https://doi.org/10.1016/0016-7037(96)00091-9.
Castillo, S., de la Rosa, J.D., Sánchez de la Campa, A.M., González-Castanedo, Y., Fernández-Caliani, J.C., Gonzalez, I., Romero, A., 2013. Contribution of mine wastes to atmospheric metal deposition in the surrounding area of an abandoned heavily polluted mining district (Rio Tinto mines, Spain). Sci. Total Environ. 449, 363–372. https://doi.org/10.1016/j.scitotenv.2013.01.076.
Chiang, K.Y., Lin, K.C., Lin, S.C., Chang, T.-K., Wang, M.K., 2010. Arsenic and lead (beudantite) contamination of agricultural rice soils in the Guandu Plain of northern Taiwan. J. Hazard. Mater. 181 (1-3), 1066–1071. https://doi.org/10.1016/j.jhazmat.2010.05.123.
Climate-data.org, 2012. Minas de Riotinto Climate.
Courtin-Nomade, A., Neel, C., Bril, H., Davranche, M., 2002. Trapping and mobilisation of arsenic and lead in former mine tailings –Environmental conditions effects. Bulletin de la Société Géologique de France 173, 479–485. https://doi.org/10.2113/173.5.479.
Couture, R.M., Charlet, L., Markelova, E., Madé, B., Parsons, C.T., 2015. On-off mobilization of contaminants in soils during redox oscillations. Environmental Science and Technology 49, 3015–3023. https://doi.org/10.1021/es5061879.
Courtin-Nomade, A., Waltzing, T., Evrard, C., Soubrand, M., Lenain, J.F., Ducloux, E., Ghorbel, S., Grosbois, C., Bril, H., 2016. Arsenic and lead mobility: From tailing materials to the aqueous compartment. Appl. Geochem. 64, 10–21. https://doi.org/10.1016/j.apgeochem.2015.11.002.
Cruz-Hernández, P., Pérez-López, R., Parviainen, A., Lindsay, M.B.J., Nieto, J.M., 2016. Trace element-mineral associations in modern and ancient iron terraces in acid drainage environment. Catena (Amst) 147. https://doi.org/10.1016/j.catena.2016.07.049.
Csavina, J., Field, J., Taylor, M.P., Gao, S., Landázuri, A., Betterton, E.A., Sáez, A.E., 2012. A review on the importance of metals and metalloids in atmospheric dust and aerosol from mining operations. Sci. Total Environ. 433, 58–73. https://doi.org/10.1016/j.scitotenv.2012.06.013.
Decreto 18/2015, 2015. Decreto 18/2015, de 27 de enero, por el que se aprueba el reglamento que regula el régimen aplicable a los suelos contaminados (Decree 18/2015, on 27th of January 2015, approving the regulation that regulates the regime applicable for contaminated soils. Junta de Andalucía, https://www.juntadeandalucia.es/boja/2015/38/3.
Díez, M., Simón, M., Martín, F., Dorronsoro, C., García, I., Van Gestel, C.A.M., 2009. Ambient trace element background concentrations in soils and their use in risk assessment. Sci. Total Environ. 407 (16), 4622–4632. https://doi.org/10.1016/j.scitotenv.2009.05.012.
Ettler, V., 2015. Soil contamination near non-ferrous metal smelters: A review. Appl. Geochem. 64, 56–74. https://doi.org/10.1016/j.apgeochem.2015.09.020.
Fernández Caliani, J.C., 2008. Una Aproximación al Conocimiento del Impacto Ambiental de la Minería en la Faja Pirítica Ibérica. Revista de la Sociedad Española de Mineralogía 10, 24–28.
Fernández-Caliani, J.C., 2012. Risk-based assessment of multimetallic soil pollution in the industrialized peri-urban area of Huelva, Spain. Environ. Geochem. Health 34 (1), 123–139. https://doi.org/10.1007/s10653-011-9396-0.
Fernández-Caliani, J.C., de la Rosa, J.D., Sánchez de la Campa, A.M., González-Castanedo, Y., Castillo, S., 2013. Mineralogy of atmospheric dust impacting the Rio Tinto mining area (Spain) during episodes of high metal deposition. Mineral. Mag. 77 (6), 2793–2810. https://doi.org/10.1180/minmag.2013.077.6.07.
Fernández-Navarro, P., García-Pérez, J., Ramis, R., Boldo, E., López-Abente, G., 2017. Industrial pollution and cancer in Spain: An important public health issue. Environ. Res. 159, 555–563. https://doi.org/10.1016/j.envres.2017.08.049.
Fernández-Navarro, P., García-Pérez, J., Ramis, R., Boldo, E., López-Abente, G., 2012. Proximity to mining industry and cancer mortality. Sci. Total Environ. 435–436, 66–73. https://doi.org/10.1016/j.scitotenv.2012.07.019.
Forray, F.L., Smith, A.M.L., Navrotsky, A., Wright, K., Hudson-Edwards, K.A., Dubbin, W.E., 2014. Synthesis, characterization and thermochemistry of synthetic Pb-As, Pb-Cu and Pb-Zn jarosites. Geochim. Cosmochim. Acta 127, 107–119. https://doi.org/10.1016/j.gca.2013.10.043.
Galán, E., Fernández-Caliani, J.C., González, I., Aparicio, P., Romero, A., 2008. Influence of geological setting on geochemical baselines of trace elements in soils. Application to soils of South-West Spain. J. Geochem. Explor. 98 (3), 89–106. https://doi.org/10.1016/j.gexplo.2008.01.001.
Gieré, R., Sidenko, N.V., Lazareva, E.V., 2003. The role of secondary minerals in controlling the migration of arsenic and metals from high-sulfide wastes (Berikul gold mine, Siberia). Appl. Geochem. 18 (9), 1347–1359. https://doi.org/10.1016/S0883-2927(03)00055-6.
González-Grijalva, B., Meza-Figueroa, D., Romero, F.M., Robles-Morúa, A., Meza-Montenegro, M., García-Rico, L., Ochoa-Contreras, R., 2019. The role of soil mineralogy on oral bioaccessibility of lead : Implications for land use and risk assessment. Sci. Total Environ. 657, 1468–1479. https://doi.org/10.1016/j.scitotenv.2018.12.148.
Guney, M., Bourges, C.-J., Chapuis, R.P., Zagury, G.J., 2017. Lung bioaccessibility of As, Cu, Fe, Mn, Ni, Pb, and Zn in fine fraction (< 20 μm) from contaminated soils and mine tailings. Sci. Total Environ. 579, 378–386. https://doi.org/10.1016/j.scitotenv.2016.11.086.
Han, Q., Wang, M., Cao, J., Gui, C., Liu, Y., He, X., He, Y., Liu, Y., 2020. Health risk assessment and bioaccessibilities of heavy metals for children in soil and dust from urban parks and schools of Jiaozuo, China. Ecotoxicol. Environ. Safety 191, 110157. https://doi.org/10.1016/j.ecoenv.2019.110157.
Hudson-Edwards, K.A., 2019. Uptake and release of arsenic and antimony in alunite-jarosite and beudantite group minerals. Am. Mineral. 104, 633–640 https://doi.org/https://doi.org/10.2138/am-2019-6591.
IARC, 1989. Some organic solvents, resin monomers and related compounds. In: Pigments and Occupational Exposures in Paint Manufacture and Painting, 47. International Agency for Research on Cancer, Lyon, France, p. 554.
Kabata-Pendias, A., 2010. Trace Elements in Soils and Plants, 4th editio. ed. CRC Press.
Kocourková, E., Sracek, O., Houzar, S., Cempírek, J., Losos, Z., Filip, J., Hršelová, P., 2011. Geochemical and mineralogical control on the mobility of arsenic in a waste rock pile at Dlouhá Ves, Czech Republic. J. Geochem. Explor. 110 (2), 61–73. https://doi.org/10.1016/j.gexplo.2011.02.009.
Kolitsch, U., Pking, A., 2001. Crystal chemistry of the crandallite, beudantite and alunite groups: A reéiew and eéaluation of the suitability as storage materials for toxic metals. J. Mineral. Petrol. Sci. https://doi.org/10.2465/jmps.96.67.
Li, G., Sun, G.-X., Ren, Y., Luo, X.-S., Zhu, Y.-G., 2018. Urban soil and human health: a review. Eur. J. Soil Sci. 69 (1), 196–215. https://doi.org/10.1111/ejss.12518.
Mazinanian, N., Hedberg, Y., Odnevall Wallinder, I., 2013. Nickel release and surface characteristics of fine powders of nickel metal and nickel oxide in media of relevance for inhalation and dermal contact. Regul. Toxicol. Pharm. 65 (1), 135–146. https://doi.org/10.1016/j.yrtph.2012.10.014.
McLean, J.E., Bledsoe, B.E., 1992. Behavior of metals in soils, EPA, Ground. ed. US EPA, Washington.
Meunier, L., Walker, S.R., Wragg, J., Parsons, M.B., Koch, I., Jamieson, H.E., Reimer, K.J., 2010. Effects of soil composition and mineralogy on the bioaccessibility of arsenic from tailings and soil in gold mine districts of nova scotia. Environ. Sci. Technol. 44 (7), 2667–2674. https://doi.org/10.1021/es9035682.
Morais, M.A., Gasparon, M., Delbem, I.D., Caldeira, C.L., Freitas, E.T.F., Ng, J.C., Ciminelli, V.S.T., 2019. Gastric/lung bioaccessibility and identification of arsenic-bearing phases and sources of fine surface dust in a gold mining district. Sci. Total Environ. 689, 1244–1254. https://doi.org/10.1016/j.scitotenv.2019.06.394.
Monaci, F., Trigueros, D., Mingorance, M.D., Rossini-Oliva, S., 2020. Phytostabilization potential of Erica australis L. and Nerium oleander L.: a comparative study in the Riotinto mining area (SW Spain). Environ. Geochem. Health 42 (8), 2345–2360. https://doi.org/10.1007/s10653-019-00391-7.
Néel, C., Bril, H., Courtin-Nomade, A., Dutreuil, J.-P., 2003. Factors affecting natural development of soil on 35-year-old sulphide-rich mine tailings. Geoderma 111 (1-2), 1–20. https://doi.org/10.1016/S0016-7061(02)00237-9.
Nieto, J.M., Capitán, M.A., Sáez, R., Almodóvar, G.R., 2003. Beudantite: A natural sink for As and Pb in sulphide oxidation processes. Trans. Inst. Min. Metall., Section B: Appl. Earth Sci. 112 (3), 293–296. https://doi.org/10.1179/037174503225003134.
Nocete, F., Sáez, R., Bayona, M.R., Nieto, J.M., Peramo, A., López, P., Gil-Ibarguchi, J.I., Inácio, N., García, S., Rodríguez, J., 2014. Gold in the Southwest of the Iberian Peninsula during the 3rd Millennium BC. J. Archaeol. Sci. 41, 691–704. https://doi.org/10.1016/j.jas.2013.10.006.
Oberdörster, G., Maynard, A., Donaldson, K., Castranova, V., Fitzpatrick, J., Ausman, K., Carter, J., Karn, B., Kreyling, W., Lai, D., Olin, S., Monteiro-Riviere, N., Warheit, D., Yang, H., 2005. Principles for characterizing the potential human health effects from exposure to nanomaterials: Elements of a screening strategy. Part. Fibre Toxicol. 2, 1–35. https://doi.org/10.1186/1743-8977-2-8.
Parviainen, A., Cruz-Hernández, P., Pérez-López, R., Nieto, J.M., Delgado-López, J.M., 2015. Raman identification of Fe precipitates and evaluation of As fate during phase transformation in Tinto and Odiel River Basins. Chem. Geol. 398, 22–31. https://doi.org/10.1016/j.chemgeo.2015.01.022.
Parviainen, A., Marchesi, C., Suárez-Grau, J.M., Garrido, C.J., Pérez-López, R., Nieto, J.M., Cobo-Cárdenas, G., 2018. Unraveling the impact of chronic exposure to metal pollution through human gallstones. Sci. Total Environ. 624, 1031–1040. https://doi.org/10.1016/j.scitotenv.2017.12.224.
Parviainen, A., Suárez-Grau, J.M., Pérez-López, R., Nieto, J.M., Garrido, C.J., Cobo-Cárdenas, G., 2016. Combined microstructural and mineralogical phase characterization of gallstones in a patient-based study in SW Spain - Implications for environmental contamination in their formation. Sci. Total Environ. 573, 433–443. https://doi.org/10.1016/j.scitotenv.2016.08.110.
Parviainen, A., Vázquez-Arias, A., Arrebola, J.P., Martín-Peinado, F.J., 2022. Human health risks associated with urban soils in mining areas. Environ. Res. 206, 112514. https://doi.org/10.1016/j.envres.2021.112514.
Pekov, I.V., Khanin, D.A., Yapaskurt, V.O., Pakunova, A.V., Ekimenkova, I.A., 2016. Minerals of the beudantite–segnitite series from the oxidation zone of the Berezovskoe gold deposit, middle Urals: Chemical variations, behavior of admixtures, and antimonian varieties. Geol. Ore Deposits 58 (7), 600–611. https://doi.org/10.1134/S1075701516070096.
Rivas-Martínez, S., Rivas-Sáenz, S., Penas, A., 2011. Worldwide bioclimatic classification system. Glob. Geobot. 1–638 https://doi.org/10.5616/gg110001.
Romero, F.M., Armienta, M.A., González-Hernández, G., 2007. Solid-phase control on the mobility of potentially toxic elements in an abandoned lead/zinc mine tailings impoundment, Taxco, Mexico. Appl. Geochem. 22 (1), 109–127. https://doi.org/10.1016/j.apgeochem.2006.07.017.
Romero, F.M., Prol-Ledesma, R.M., Canet, C., Alvares, L.N., Pérez-Vázquez, R., 2010. Acid drainage at the inactive Santa Lucia mine, western Cuba: Natural attenuation of arsenic, barium and lead, and geochemical behavior of rare earth elements. Appl. Geochem. 25 (5), 716–727. https://doi.org/10.1016/j.apgeochem.2010.02.004.

Rossini-Oliva, S., Mingorance, M.D., Monaci, F., Valdés, B., 2016. Ecophysiological indicators of native Cistus ladanifer L. at Riotinto mine tailings (SW Spain) for assessing its potential use for rehabilitation. Ecol. Eng. 91, 93–100. https://doi.org/10.1016/j.ecoleng.2016.01.078.

Roussel, C., Néel, C., Bril, H., 2000. Minerals controlling arsenic and lead solubility in an abandoned gold mine tailings. Sci. Total Environ. 263 (1-3), 209–219. https://doi.org/10.1016/S0048-9697(00)00707-5.

Sáez, R., Pascual, E., Toscano, M., Almodóvar, G.R., 1999. The Iberian type of volcano-sedimentary massive sulphide deposits. Miner. Deposita 34 (5-6), 549–570. https://doi.org/10.1007/s001260050220.

Sánchez de la Campa, A.M., Sánchez-Rodas, D., Márquez, G., Romero, E., de la Rosa, J. D., 2020. 2009–2017 trends of PM10 in the legendary Riotinto mining district of SW Spain. Atmos. Res. 238, 104878. https://doi.org/10.1016/j.atmosres.2020.104878.

Schlesinger, R.B., Kunzli, N., Hidy, G.M., Gotschi, T., Jerrett, M., 2006. The Health Relevance of Ambient Particulate Matter Characteristics: Coherence of Toxicological and Epidemiological Inferences. Inhalation Toxicol. 18 (2), 95–125. https://doi.org/10.1080/08958370500306016.

Schwertmann, U., 1991. Solubility and dissolution of iron oxides. Plant Soil 130 (1-2), 1–25. https://doi.org/10.1007/BF00011851.

Sejkora, J., Škovíra, J., Čejka, J., Plášil, J., 2009. Cu-rich members of the beudantite-segnitite series from the krupka ore district, the krušné hory mountains, Czech Republic. J. Geosci. 54, 355–371. https://doi.org/10.3190/jgeosci.055.

Simón, M., Dorronsoro, C., Ortiz, I., Martín, F., Aguilar, J., 2002. Pollution of carbonate soils in a Mediterranean climate due to a tailings spill. Eur. J. Soil Sci. 53, 321–330. https://doi.org/10.1046/j.1365-2389.2002.00435.x.

Simón, M., Martín, F., García, I., Bouza, P., Dorronsoro, C., Aguilar, J., 2005. Interaction of limestone grains and acidic solutions from the oxidation of pyrite tailings. Environ. Pollut. 135 (1), 65–72. https://doi.org/10.1016/j.envpol.2004.10.013.

Tchounwou, P.B., Yedjou, C.G., Patlolla, A.K., Sutton, D.J., 2012. Heavy metal toxicity and the environment, in: Molecular, Clinical and Environmental Toxicology. Experientia Supplementum, Vol. 101. pp. 133–164. https://doi.org/10.1007/978-3-7643-8340-4_6.

Tornos, F., 2006. Environment of formation and styles of volcanogenic massive sulfides: The Iberian Pyrite Belt. Ore Geol. Rev. 28 (3), 259–307. https://doi.org/10.1016/j.oregeorev.2004.12.005.

U.S.EPA, 2006. XRF technologies for measuring trace elements in soil and sediment. Niton XLt 700 Series XRF Analyzer. Washington, D.C.

U.S.EPA, 1996. Air quality criteria for particulate matter, vol. I. US Environmental Protection Agency, EPA Report No. EPA 600/P-95/001aF.

Valavanidis, Athanasios, Fiotakis, Konstantinos, Vlachogianni, Thomais, 2008. Airborne particulate matter and human health: Toxicological assessment and importance of size and composition of particles for oxidative damage and carcinogenic mechanisms. J. Environ. Sci. Health - Part C Environ. Carcinogen. Ecotoxicol. Rev. 26 (4), 339–362. https://doi.org/10.1080/10590500802494538.

WHO, 2000. Chapter 7.3. Particulate matter. In: Air quality guidelines for Europe. 2nd Edition. WHO Regional Publications, European Series, No. 91. Copenhagen, Denmark.

Zereini, F., Wiseman, C.L.S., Püttmann, W., 2012. In vitro investigations of platinum, palladium, and rhodium mobility in urban airborne particulate matter (PM10, PM2.5, and PM1) using simulated lung fluids. Environ Sci Technol 46, 10326–10333 https://doi.org/10.1021/es3020887.

Zhang, H., Mao, Z., Huang, K., Wang, X., Cheng, L., Zeng, L., Zhou, Y., Jing, T., 2019. Multiple exposure pathways and health risk assessment of heavy metal(loid)s for children living in fourth-tier cities in Hubei Province. Environ. Int. 129, 517–524. https://doi.org/10.1016/j.envint.2019.04.031.

Zuluaga, M.C., Norini, G., Ayuso, R., Nieto, J.M., Lima, A., Albanese, S., De Vivo, B., 2017. Geochemical mapping, environmental assessment and Pb isotopic signatures of geogenic and anthropogenic sources in three localities in SW Spain with different land use and geology. J. Geochem. Explor. 181, 172–190. https://doi.org/10.1016/j.gexplo.2017.07.011.